PAPER

Directly determining ^{143}Nd/^{144}Nd isotope ratios using thermal ionization mass spectrometry for geological samples without separation of Sm–Nd

Chao-feng Li,[*ab] **Xian-hua Li,**[a] **Qiu-li Li,**[a] **Jing-hui Guo**[a] **and Xiang-hui Li**[a]

Sm–Nd isotopic system is a powerful tracer and dating tool in geochemistry and cosmochemistry. Thermal ionization mass spectrometry (TIMS) is the benchmark method for obtaining high precision Nd isotope ratios. Traditionally, a two-step separation was employed in order to obtain high purity Nd fraction, which makes the sample preparation time-consuming. In this study, we present a new method to directly obtain precise and accurate Nd isotope ratios of geological samples without Sm–Nd separation. The key point is to well correct isobaric interferences of ^{144}Sm on ^{144}Nd for this method. The accurate intensity of ^{144}Sm can be obtained using ^{147}Sm/^{144}Sm ratio of 4.87090 and mass discrimination factor of Sm (β_{Sm}), which is achieved using ^{147}Sm/^{149}Sm ratio of 1.08583 with Russell equation. Consequently, the real intensity of ^{144}Nd was achieved, then also raw ^{146}Nd/^{144}Nd, ^{143}Nd/^{144}Nd ratios. Finally, ^{143}Nd/^{144}Nd ratio is normalized using ^{146}Nd/^{144}Nd ratio of 0.7219 following exponential law. The accuracy of this method is validated by replicating TIMS measurements for thirteen international reference materials of silicate rock, spanning a wide range of Sm/Nd from 0.13 to 0.46 and bulk compositions. The measured ^{143}Nd/^{144}Nd ratios of the rock standards are in good agreement with the reported values of within error of $\pm0.004\%$. Our new method shortens the analytical procedure and significantly improves sample throughput which greatly contributes to those studies requiring a large dataset and quick analysis.

1. Introduction

Samarium-neodymium isotopic system has been widely applied to geochemical and geochronological studies.[1,2] The natural variation in the ^{143}Nd/^{144}Nd isotope ratio is small and derived from the radioactive decay of ^{147}Sm to ^{143}Nd (half life = 106 billion years). Therefore, in order to utilize this isotopic tracer, high precision Nd isotopic measurement better than (0.005%) is required. Multiple-collector thermal ionization mass spectrometry (TIMS) and multiple-collector inductively coupled plasma mass spectrometry (MC-ICP-MS) is currently used[3–27] for the precise measurement of neodymium isotope ratios, with internal and external precisions of *ca.* 0.002% and *ca.* 0.005%, respectively.

Although MC-ICP-MS demonstrates more efficiency in sample throughput than the TIMS method,[3,6,20] TIMS has higher sensitivity and accuracy for Nd isotopic ratio than MC-ICP-MS.[7–13] In previous research,[7–26] precise measurements of Nd isotopic ratios by TIMS require efficient separation of Nd from matrix solution to eliminate complex matrix effect and isobaric interference of light rare earth elements (REEs). Conventional separation scheme is performed in a two-step column chromatography method.[7–26] The first step is to separate REEs from matrix solution by classical cation-exchange resin, and the second step is to purify Nd fraction from the REEs in order to minimize the isobaric interference by reversed-phase chromatographic methods or high performance liquid chromatography (HPLC) methods. This separation work is time-consuming and tedious making a variety of research more difficult. This is especially true for the case when a large number of data are necessary such as researches on paleo-environment and sediment geology.

In this study, we present a method of directly measuring ^{143}Nd/^{144}Nd isotope ratio in REEs fraction by Triton TIMS with a simplified chemical separation procedure. After carrying out matrix separation using a cation-exchanger resin chromatography, we did not perform the second step to separate Nd from REEs. However, precise and accurate ^{143}Nd/^{144}Nd data can still be achieved to the level of high purity Nd in past researches,[7–26] as shown by the measurement of natural silicate rock samples with a wide range of Sm/Nd (0.13–0.46) and bulk compositions (from felsic to mafic rocks). This allows a large data throughput which can be potentially applied to the studies requiring large datasets and quick analysis.

2. Experimental

2.1 Reagents and materials

Re ribbon: 0.035 mm thick, 0.77 mm wide and 99.98% pure, H. Cross Company.

[a]*State Key Laboratory of Lithospheric Evolution, Institute of Geology and Geophysics, Chinese Academy of Sciences, Beijing, 100029, China. E-mail: cfli@mail.iggcas.ac.cn; Fax: +86 10 62010846; Tel: +86 10 82998583*
[b]*School of Earth Sciences, Graduate University of Chinese Academy of Sciences, Beijing, 100039, China*

Milli-Q H_2O: 18.2 MΩ cm^{-1} at 25 °C.

HCl, HF, HNO_3, $HClO_4$: Purified by sub-boiling distillation using Savillex Teflon distillers.

H_3PO_4: Purified using cation exchange chromatographic methods.

JNdi-1: Neodymium isotopic international reference and 99.999% pure; JNdi-1 solutions of 200 ppm

LRIG: Neodymium isotopic work reference and 99.99% pure; LRIG solutions of 200 ppm

Sm_2O_3: 99.99% pure; Sm solutions of 200 ppm

$BaCl_2$: 99.99% pure; Ba solutions of 10 000 ppm

Cation exchange column: 7 cm long × 6 mm i.d. with a 30 mL reservoir, packed with Bio-Rad AG50W × 12resin (200–400 mesh), 2 mL of resin bed volume.

Rock powder reference materials from United States Geological Survey (USGS) and Geological Survey of Japan (GSJ): USGS BCR-2 (basalt), BHVO-2 (basalt), W-2 (diabase), BIR-1(basalt), GSP-2 (granodiorite); GSJ JA-3 (andesite), JR-2 (rhyolite), JR-3 (rhyolite), JG-2 (granite), JG-3 (granite), JG-1a (granite), JGb-1 (basalt) and JGb-2 (basalt).

2.2 Sample digestion and column chemistry

2.2.1 Sample digestion. All chemical preparations were conducted on special class 100 work benches inside a class 1000 clean laboratory. About 100 mg of felsic rock to mafic rock reference materials were weighed (to 0.1 mg precision) into Savillex 7.5 mL Teflon-PFA vials. The samples were dissolved on a hotplate at about 120 °C using a mixed acid of 2.5 mL 22 M HF + 1 mL 14 M HNO_3 + 0.25 mL 12.4M $HClO_4$ for one week. The dissolved sample solution was then evaporated to dryness and treated overnight with 2 mL of 6M HCl at *ca.* 90 °C. Then, the solution was dried down at *ca.* 150 °C again. Finally, the samples were dissolved with 1.1 mL of 2.5M HCl on a 90 °C hotplate overnight.

2.2.2 Column chemistry. The resulting solutions obtained from the former steps were centrifuged at 5000 rpm for 8 min and then 1 mL of the supernatant was loaded onto the pre-conditioned AG50W × 12 (200–400 mesh) resin columns for separation of REE from sample matrix. After rinsing four times with 0.5 mL of 2.5M HCl, the column was washed with 9 mL of 5M HCl. The REEs were then stripped with 7 mL of 6M HCl. Some heavy REEs (HREEs) were removed from Sm and Nd during this step, and the Sm, Nd recovery yields of this step were close to 100%. The experimental measurements required to calibrate the columns (major and trace element distribution curve), which were performed using an ICP-MS (Agilent 7500). As shown in Table 1, most matrix elements and part of HREEs had been rinsed in fraction 1 before collection of Sm–Nd fraction. Part of Ba, Sr and most of La, Ce, Pr, Gd, Tb coexisted with Sm–Nd in fraction 2. The yield of Sm and Nd were more than 90% in fraction 2. Part of Ce, Pr and most Ba, La were rinsed in fraction 3. The whole procedure blank for Nd is lower than 50 pg, rendering blank corrections insignificant.

2.3 Mass spectrometry

Nd isotopic measurements were performed on a Thermo Fisher Scientific Triton thermal ionization mass spectrometer (TIMS) at the Tianjin Institute of Geology and Mineral Resources. The instrument is equipped with a multi-collector assembly comprising one fixed central and 8 adjustable Faraday cups with a dynamic range of 50 V. An accelerating voltage of 10 kV is used for Nd isotope analysis. Faraday cup collectors are used with a 10^{11} Ω resistor for isotopic determinations. The Nd isotopic data are acquired in static collection mode and the configuration of the Faraday cups is shown in Table 2.

2.3.1 Sample loading. A double Re filament configuration was used. In past investigations,[11–13] phosphoric acid was found to be an ideal emitter for Nd isotopic measurement as Nd$^+$ by TIMS. Hence, approximately 0.5 µL of 0.13 M phosphoric acid was loaded on a zone refined and degassed Re filament (H. Cross) and dried at 0.8 A. The samples were then dissolved and loaded in 1 µL of 2.5 M HCl and dried by heating with a 0.8 A. Finally, after 0.5 µl of 0.13 M phosphoric acid was loaded and dried, the filaments were heated to a dull red glow at *ca.* 2 A for a few seconds. In order to investigate the feasibility of direct measurement of $^{143}Nd/^{144}Nd$ ratio, two mixed JNdi-1 and LRIG standards were prepared. In each TIMS measurement, 200ng of JNdi-1 and LRIG mixed standard solutions were loaded onto an area as small as possible on the Re filaments (about 1 mm × 0.7 mm square), respectively.

Table 1 Sample purity and recovery of Sm and Nd[a,b,c]

Elements	Fraction 1 (%)	Fraction 2 (%)	Fraction 3 (%)
Na	100	0	0
Mg	100	0	0
Al	100	0	0
K	100	0	0
Ca	100	0	0
Ti	100	0	0
Mn	100	0	0
Fe	99.9	0.1	0
Y	98.4	1.6	0
Rb	100	0	0
Sr	93.2	6.8	0
Ba	2.3	9.4	88.3
La	5.3	20.6	74.1
Ce	2.7	57.6	39.7
Pr	3.3	84.3	12.4
Nd	3.5	94.4	2.1
Sm	2.9	96.2	0.9
Gd	9.9	87.9	2.3
Tb	31.0	68.7	0.3
Ho	94.5	5.5	0
Er	98.0	2.0	0
Tm	99.8	0.2	0
Yb	98.9	0.9	0.2
Lu	98.8	0.8	0.4
Hf	99.6	0.4	0

[a] Fraction 1: 3 ml 2.5M HCL(1 ml loading + 2 ml rinsing) + 9 ml 5.0M HCL (rinsing). [b] Fraction 2: 7 ml 6.0M HCL (rinsing). [c] Fraction 3: 10 ml 6.0M HCL (rinsing).

Table 2 Cup setting of static multi-collector mode

Cup	L4	L3	L2	L1	CC	H1
	^{143}Nd	^{144}Nd	^{145}Nd	^{146}Nd	^{147}Sm	^{149}Sm

This journal is © The Royal Society of Chemistry 2011

J. Anal. At. Spectrom., 2011, **26**, 2012–2022 | 2013

2.3.2 Nd isotope measurement method. Nd isotope ratios were measured as the metal ion manner using a double rhenium filament assembly. The amplifier gain of each Faraday cup was calibrated twice everyday. The background was monitored at masses 146.5 in the center cup in static collection mode during data acquisition. When the ion source vacuum was better than 1.5×10^{-7} mbar, the measurement of Nd^+ ion beams could be started. The ionization filament was first heated at a rate of 400 mA min^{-1} to a temperature of 1700 °C and the final current of ionization filament reached 4.5 A. The evaporation filament was then heated at a rate of 200 mA min^{-1} until a signal of 0.02×10^{-11} A for ^{143}Nd was obtained. The beam was roughly focused and the evaporation filament was slowly heated to obtain an ion current of $0.8–1 \times 10^{-11}$ A for ^{143}Nd. Then, the beam was refocused until an optimum intensity was reached. Faraday baselines were measured for 33 s at the beginning of every block by deflecting the beams using the x-symmetry lens and a peak-center routine was run, prior to the start of an analysis. Data were collected for 9–12 blocks with each block containing 15 cycles that, in turn, consisted of 4 s of integration time. The total analytical time for each measurement was about 50 min.

The data reduction has been performed "off-line" including isobaric interference corrections and then mass fractionation corrections. Instrumental mass discrimination was corrected by using the natural constant $^{146}Nd/^{144}Nd$ ratio (0.7219) as an internal standard after isobaric interference correction of ^{144}Sm on ^{144}Nd was corrected using interference-free $^{147}Sm/^{149}Sm$ ratio for mass fractionation. The international standard, JNdi-1 Nd, was employed to evaluate instrument stability during analytical session. During the period of data collection, the average value measured for the JNdi-1 was 0.512102 ± 9 (2 SD, $N = 8$) for $^{143}Nd/^{144}Nd$, which was in good agreement with the reported value of 0.512115[27] within error ($\pm0.005\%$, 2 RSD).

Subtracted and corrected isobaric interferences from Sm were conducted using eqn (1) and eqn (2). Prior to Nd normalization using $^{146}Nd/^{144}Nd$ ratio of 0.7219[4–13,16–26] the interference-free $^{147}Sm/^{149}Sm$ ratio was measured to determine Sm mass discrimination (β_{Sm}) using a $^{147}Sm/^{149}Sm$ ratio of 1.08583.[28] Then, the isobaric correction of ^{144}Sm on ^{144}Nd was calculated using a $^{147}Sm/^{144}Sm$ ratio of 4.87090.[28] Afterwards, $^{143}Nd/^{144}Nd$ and $^{145}Nd/^{144}Nd$ ratios were corrected using $^{146}Nd/^{144}Nd$ ratio of 0.7219 following eqn (3)–(8).

$$\beta_{Sm} = Ln([^{147}Sm/^{149}Sm]_t/[^{147}Sm/^{149}Sm]_m)/Ln[M_{147}/M_{149}] \quad \text{(Equation 1)}$$

$$[^{144}Nd]_c = [^{144}(Nd+Sm)]_m - [^{147}Sm]_m/[^{147}Sm/^{144}Sm]_t \times [M_{147}/M_{144}]^{\beta Sm} \quad \text{(Equation 2)}$$

$$[^{143}Nd/^{144}Nd]_m = [^{143}Nd]_m/[^{144}Nd]_c \quad \text{(Equation 3)}$$

$$[^{145}Nd/^{144}Nd]_m = [^{145}Nd]_m/[^{144}Nd]_c \quad \text{(Equation 4)}$$

$$[^{146}Nd/^{144}Nd]_m = [^{146}Nd]_m/[^{144}Nd]_c \quad \text{(Equation 5)}$$

$$\beta_{Nd} = Ln([^{146}Nd/^{144}Nd]_m/[^{146}Nd/^{144}Nd]_t)/Ln[M_{146}/M_{144}] \quad \text{(Equation 6)}$$

$$[^{143}Nd/^{144}Nd]_c = [^{143}Nd/^{144}Nd]_m/Power[M_{143}/M_{144}, \beta_{Nd}] \quad \text{(Equation 7)}$$

$$[^{145}Nd/^{144}Nd]_c = [^{145}Nd/^{144}Nd]_m/Power[M_{145}/M_{144}, \beta_{Nd}] \quad \text{(Equation 8)}$$

Where "m" and "c" denote the measured value and the corrected value, "t" means true value. M_{144}, M_{147} and M_{149} represent the actual mass of ^{144}Sm, ^{147}Sm and ^{149}Sm, respectively. M_{143}, M_{144}, M_{145} and M_{146} represent the actual mass of ^{143}Nd, ^{144}Nd, ^{145}Nd and ^{146}Nd, respectively. $[^{147}Sm/^{149}Sm]_t$ is 1.08583 and $[^{147}Sm/^{144}Sm]_t$ is 4.87090. We adopt 0.7219 as $[^{146}Nd/^{144}Nd]_t$ to calculate Nd mass discrimination (β_{Nd}).

3. Results and discussion

3.1 Measurements of mixed standard solution (JNdi-1 and LRIG)

Two mixed standard (JNdi-1 and LRIG) were employed to characterize a number of mixed standards using TIMS to test the accuracy and reproducibility of our TIMS approach. Regarding to preparation of the mixed standard solution, Sm_2O_3 powder was dissolved using 2 M HCl and diluted to 200 ppm, then added into LRIG and JNdi-1 solution, respectively. Four mixed proportions with different Sm/Nd (0.3, 0.5, 0.7 and 1.0) were prepared for each mixed standard. Mixed standard solutions with Sm/Nd = 0.3, 0.5 and 0.7 were measured in 12 runs, whereas mixed standard solutions with Sm/Nd = 1.0 were conducted in 8 runs. Analytical data are listed in Table 3 and 4. As shown in Fig. 1a and 1b, typical internal precision with 3–5 ppm and external precision with 11–12 ppm was achieved. Forty-four replicated measurements of mixed JNdi-1 and mixed LRIG yielded a $^{143}Nd/^{144}Nd$ value of 0.512112 ± 0.000011 (2 SD) and 0.512197 ± 0.000012 (2 SD), respectively, which were in good agreement with the reported values of 0.512115 for JNdi-1[27] and 0.512203 for LRIG.[9] The results from the above different mixed standard with different Sm/Nd ratios indicated that our method was effective for samples with Sm/Nd ratio lower than 1.0.

3.2 Relationship between isotopic fractionation (β_{Sm} and β_{Nd}) and signal intensities

The relationship among βSm, βNd and the intensity variation of ^{147}Sm and ^{143}Nd should be carefully investigated in order to know this method further. In most cases, typical intensity of ^{147}Sm and ^{143}Nd were higher than 300mV and 800mV respectively. Generally, their intensities decrease or increase simultaneously, because Sm and Nd have similar ionization temperature.

A typical run in a mixed JNdi-1(No.16 in Table 3) with Sm/Nd of 0.5 was employed to illustrate above relationship. This run included 150 cycles, with 1 cycle being rejected due to anomalous deviation. As shown in Fig. 2a, the variation in intensity of ^{143}Nd and ^{147}Sm was 1390~1870 mV and 420~594 mV, respectively. Raw $^{143}Nd/^{144}(Nd + Sm)$ ratios showed wide range from 0.4953 to 0.4961. However, the corrected $^{143}Nd/^{144}Nd$ ratios were accurate and not affected by the intensity of ^{147}Sm, yielded a mean value of 0.512108 ± 0.000004 (2 SE, $N = 149$ cycles). The relationship between β_{Sm} and β_{Nd} is shown in Fig. 2b. Obviously, β_{Sm} was significantly higher than β_{Nd} in each cycle. This phenomena was typical and widely existed in other samples (Table 3, 4, 5). Furthermore, β_{Sm}/β_{Nd} ratios were unstable and showed large variety. The β_{Sm}/β_{Nd} ratios showed a decreasing trend with time

Table 3 Measurements of mixed standard JNdi-1[a]

Mixed JNdi-1	β_{Sm}	β_{Nd}	$^{143}Nd/^{144}Nd$ (±S.E)	$^{145}Nd/^{144}Nd$ (±S.E)	Sm/Nd
1*	0.270	0.023	0.512101(3)	0.348406(2)	0.3
2*	0.270	0.042	0.512110(5)	0.348408(3)	0.3
3*	0.223	0.028	0.512107(3)	0.348407(2)	0.3
4*	0.299	0.063	0.512105(4)	0.348412(3)	0.3
5*	0.306	0.043	0.512105(4)	0.348409(2)	0.3
6*	0.295	0.074	0.512104(4)	0.348409(3)	0.3
7	0.276	0.021	0.512106(3)	0.348405(2)	0.3
8	0.373	0.136	0.512108(3)	0.348413(2)	0.3
9	0.306	0.060	0.512101(3)	0.348409(2)	0.3
10	0.247	0.028	0.512113(3)	0.348405(1)	0.3
11	0.276	0.046	0.512102(4)	0.348408(2)	0.3
12	0.241	0.037	0.512107(3)	0.348407(2)	0.3
13*	0.284	0.051	0.512113(3)	0.348408(2)	0.5
14*	0.187	0.090	0.512113(3)	0.348406(2)	0.5
15*	0.300	0.060	0.512108(4)	0.348413(3)	0.5
16*	0.211	0.057	0.512108(3)	0.348411(2)	0.5
17*	0.319	0.064	0.512113(5)	0.348407(3)	0.5
18*	0.265	0.011	0.512109(3)	0.348408(2)	0.5
19	0.148	0.103	0.512115(4)	0.348414(2)	0.5
20	0.339	0.075	0.512114(8)	0.348417(5)	0.5
21	0.231	0.035	0.512114(4)	0.348407(2)	0.5
22	0.117	0.124	0.512113(4)	0.348409(2)	0.5
23	0.231	0.046	0.512114(4)	0.348413(2)	0.5
24	0.231	0.046	0.512114(4)	0.348412(2)	0.5
25*	0.239	0.035	0.512118(4)	0.348409(2)	0.7
26*	0.282	0.030	0.512113(4)	0.348408(3)	0.7
27*	0.310	0.072	0.512116(4)	0.348411(3)	0.7
28*	0.144	0.086	0.512115(5)	0.348407(3)	0.7
29*	0.238	0.019	0.512109(4)	0.348408(3)	0.7
30*	0.287	0.033	0.512113(4)	0.348406(3)	0.7
31	0.268	0.020	0.512112(5)	0.348410(3)	0.7
32	0.224	0.034	0.512119(4)	0.348411(2)	0.7
33	0.268	0.035	0.512116(4)	0.348409(3)	0.7
34	0.287	0.037	0.512116(5)	0.348403(4)	0.7
35	0.295	0.053	0.512119(4)	0.348405(3)	0.7
36	0.137	0.123	0.512113(6)	0.348408(4)	0.7
37*	0.202	0.027	0.512121(3)	0.348414(10)	1.0
38*	0.313	0.083	0.512118(3)	0.348410(2)	1.0
39*	0.312	0.040	0.512119(4)	0.348409(3)	1.0
40*	0.400	0.151	0.512114(4)	0.348409(3)	1.0
41*	0.255	0.027	0.512119(4)	0.348412(2)	1.0
42*	0.274	0.039	0.512121(5)	0.348414(2)	1.0
43	0.302	0.034	0.512114(3)	0.348411(2)	1.0
44	0.335	0.077	0.512117(5)	0.348410(3)	1.0
Mean ± 2SD	0.264	0.055	0.512112(11)	0.348409(6)	

[a] Note: Number* was employed to plot Fig. 5 and test the feasibility of $[^{147}Sm/^{149}Sm]_t$ and $[^{147}Sm/^{144}Sm]_t$.

in this analysis session, whereas such phenomena was not typical for other samples. Sometimes, β_{Sm}/β_{Nd} ratios showed a relative stable or increasing trend with time in other samples. This is distinguished from what is shown in MC-ICP-MS analysis,[6] where the ratios are stable and a little high.

The different ionization mechanism leads to these different experimental phenomena. The ICP source allowed almost complete ionization of Sm and Nd at atmospheric pressures, although showing large but relatively stable mass discrimination. In contrast, for TIMS, the solid samples are loaded on a metal filament and, then evaporated and ionized with slowly increasing surface temperature of filament. Hence, TIMS devices allowed selective ionization of specific element species and exhibited less but changing mass fractionation. It was well-known that the optimal ionization temperature of Sm was lower than that of Nd. Hence, part of Sm had been evaporated and ionized prior to

performing measurements of Nd. This generated β_{Sm} obviously larger than β_{Nd} during evaporation of sample from the same filament in general. In addition, loading methods, matrix elements, vacuum condition and speed of tuning filament current were also important factors affecting β_{Sm} and β_{Nd}.

3.3 Results of certificated reference materials (CRMs) from USGS and GSJ

$^{143}Nd/^{144}Nd$ isotope ratios of thirteen CRMs from USGS and GSJ were measured to further examine the accuracy and precision of our method. These standards covered a wide range of major element composition (from mafic to felsic) and Sm/Nd (0.13–0.46). Rock samples were digested and purified using chemical procedure described above without further Sm and Nd separation. As shown in Table 5, when Sm was corrected using

This journal is © The Royal Society of Chemistry 2011

J. Anal. At. Spectrom., 2011, **26**, 2012–2022 | 2015

Table 4 Measurements of mixed standard LRIG

Mixed LRIG	β_{Sm}	β_{Nd}	$^{143}Nd/^{144}Nd$ ($\pm$S.E)	$^{145}Nd/^{144}Nd$ ($\pm$S.E)	Sm/Nd
1	0.212	0.024	0.512200(3)	0.348411(2)	0.3
2	0.177	0.069	0.512200(3)	0.348414(2)	0.3
3	0.176	0.054	0.512189(4)	0.348414(3)	0.3
4	0.131	0.112	0.512197(4)	0.348409(2)	0.3
5	0.205	0.044	0.512197(4)	0.348414(3)	0.3
6	0.145	0.082	0.512189(5)	0.348406(3)	0.3
7	0.217	0.041	0.512202(5)	0.348412(2)	0.3
8	0.213	0.026	0.512210(6)	0.348414(4)	0.3
9	0.234	0.023	0.512200(4)	0.348414(3)	0.3
10	0.191	0.041	0.512196(4)	0.348409(3)	0.3
11	0.221	0.026	0.512194(4)	0.348409(2)	0.3
12	0.215	0.028	0.512188(4)	0.348412(3)	0.3
13	0.155	0.077	0.512197(4)	0.348409(2)	0.5
14	0.135	0.097	0.512197(3)	0.348409(2)	0.5
15	0.261	0.018	0.512204(3)	0.348410(2)	0.5
16	0.261	0.030	0.512194(3)	0.348409(2)	0.5
17	0.213	0.045	0.512193(3)	0.348406(2)	0.5
18	0.218	0.016	0.512199(5)	0.348415(3)	0.5
19	0.180	0.064	0.512197(3)	0.348411(2)	0.5
20	0.203	0.035	0.512191(4)	0.348410(3)	0.5
21	0.176	0.074	0.512200(4)	0.348407(2)	0.5
22	0.223	0.021	0.512193(3)	0.348410(2)	0.5
23	0.208	0.027	0.512198(5)	0.348413(3)	0.5
24	0.202	0.045	0.512198(4)	0.348405(2)	0.5
25	0.198	0.042	0.512194(3)	0.348404(2)	0.7
26	0.189	0.041	0.512194(3)	0.348409(2)	0.7
27	0.251	0.021	0.512204(4)	0.348413(3)	0.7
28	0.224	0.027	0.512187(4)	0.348408(2)	0.7
29	0.176	0.049	0.512198(6)	0.348408(4)	0.7
30	0.226	0.018	0.512202(8)	0.348421(2)	0.7
31	0.193	0.063	0.512190(4)	0.348405(2)	0.7
32	0.161	0.090	0.512194(4)	0.348410(3)	0.7
33	0.224	0.024	0.512188(5)	0.348409(3)	0.7
34	0.215	0.024	0.512205(5)	0.348402(3)	0.7
35	0.173	0.062	0.512190(4)	0.348408(2)	0.7
36	0.204	0.020	0.512196(5)	0.348417(3)	0.7
37	0.193	0.013	0.512196(5)	0.348404(3)	1.0
38	0.183	0.048	0.512196(3)	0.348407(2)	1.0
39	0.143	0.056	0.512199(5)	0.348417(3)	1.0
40	0.332	0.099	0.512203(4)	0.348405(3)	1.0
41	0.196	0.023	0.512204(7)	0.348410(5)	1.0
42	0.172	0.073	0.512195(7)	0.348414(4)	1.0
43	0.182	0.045	0.512215(8)	0.348410(2)	1.0
44	0.309	0.054	0.512205(4)	0.348409(3)	1.0
Mean $\pm$ 2SD	0.203	0.046	0.512197(12)	0.348410(8)	

the aforementioned methods, the measured $^{143}Nd/^{144}Nd$ isotope ratios were in good agreement with the data measured previously by TIMS which removed Sm from Nd.[9,10,16–21,24–26] In order to further verify the reliability of our method, all CRMs were also purified using classic two-step separation method.[9,10,17–19] All samples with high purified Nd were measured by Triton. As indicated in Table 6, the results were well consistent with previous reported data and above corrected data in Table 5. Both average values of $^{143}Nd/^{144}Nd$ from purified Nd fraction in Table 6 and REEs fraction in Table 5 are plotted in Fig. 3. As can be seen in Fig. 3, they show good overlap within error for all CRMs indicating our method robustness.

The analytical reproducibility for $^{143}Nd/^{144}Nd$ ratios was evaluated using the USGS reference material BCR-2 and BIR-1. As shown in Table 5, thirteen replicated measurements of $^{143}Nd/^{144}Nd$ from BCR-2 sample yielded a $^{143}Nd/^{144}Nd$ value of 0.512630 $\pm$ 0.000010 (2 SD), well consistent with reported values 0.512622–0.512654 for BCR-2.[9,10,19–21] In addition, thirty-nine replicated measurements of $^{143}Nd/^{144}Nd$ from BCR-2 sample treated with traditional two-step procedure during one year (2009.1–2010.1) in our laboratory, yielded a $^{143}Nd/^{144}Nd$ value of 0.512634 $\pm$ 0.000026 (2 SD). There was no difference for BCR-2 standard sample within error between one-step separation and two-step separation, indicating robustness of our new method. Eight replicated measurements of $^{143}Nd/^{144}Nd$ from BIR-1 yielded a value of 0.513084 $\pm$ 0.000012 (2SD), showed good agreement with the literature values for BIR-1 (0.513060–0.513100).[9,10,16,17] Note that BIR-1 has the highest ratio of Sm/Nd (0.46) among the previously-published 93 natural silicate rock CRMs.[29,30] Thus, to precisely determine $^{143}Nd/^{144}Nd$ from BIR-1 without Sm–Nd separation is the biggest challenge to our method though both precision and reproducibility of BIR-1 are well consistent with reported values.

Several important issues must be emphasized prior to application of this method. Firstly, it is strongly recommended to adopt sandwich loading method using dilute phosphoric acid. As
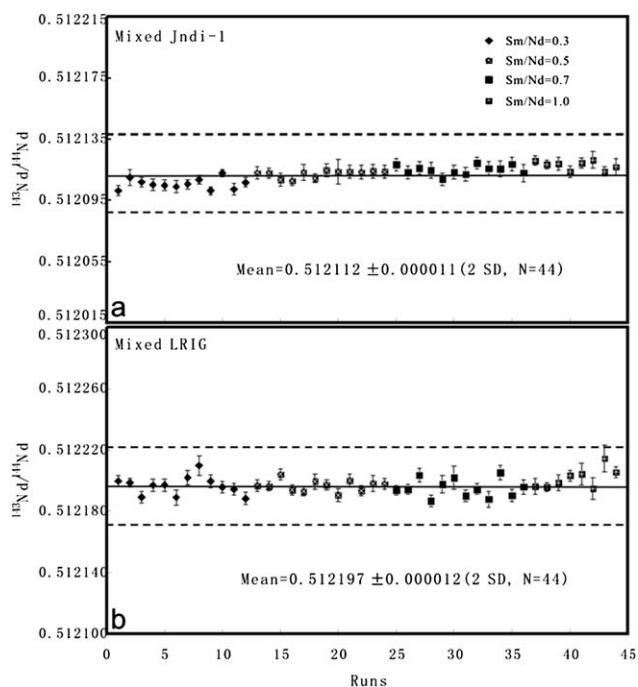
Fig. 1 ^{143}Nd/^{144}Nd measurements of mixed standard with different Sm/Nd ratios. **a.** JNdi-1; **b.** LRIG.

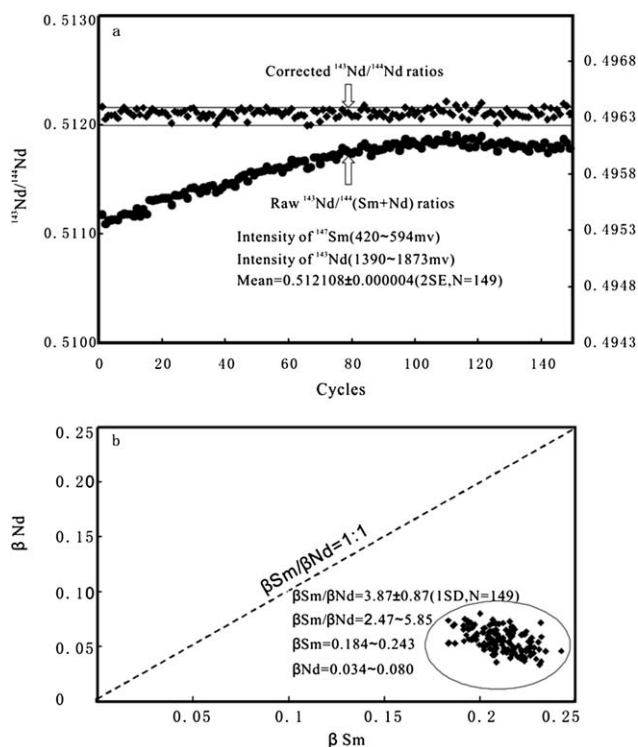**Fig. 2** A typical analysis session in a mixed Jnid-1. **a.** the raw ^{143}Nd/^{144}(Sm + Nd) and corrected ^{143}Nd/^{144}Nd for each cycle. **b.** relationship of βSm and βNd.

shown in Table 1, the sample purity achieved using one-step cation resin method had minor trace elements such as Ba, Sr and HREEs, which might slightly affect ionization efficiency of Nd on the filament. Whereas, the sandwich loading method could

provide high and stable signal intensity of Nd for a long time. For example, 3000 mv of ^{144}Nd for 300–500 ng of Nd on the Re filament could be kept for more than 10 h in previous studies.[11–13] Secondly, the ideal sample size of Nd should be larger than 100 ng for precise Nd isotopic analyses of geological samples. In general, it was necessary to weigh more than 100 mg sample in order to avoid inhomogeneity of the samples. The content of Nd in most rock samples was higher than 1 ppm. Thus, 100 mg samples provided easily more than 100 ng Nd for each analysis. Therefore, our method was suitable for most geological samples. For samples having less than 50 ng of Nd, NdO$^+$ technique combined with traditional two-step procedure is recommended because Nd could be ionized more efficiently as NdO$^+$ than as Nd$^+$ on TIMS.[7–10] Thirdly, the intensity of ^{147}Sm was recommended to maintain a reasonable level ($\geq$20 mv) so that ^{147}Sm/^{149}Sm and β_{Sm} can be measured precisely to correct the isobaric interference of ^{144}Sm on ^{144}Nd. In most cases, the intensity of ^{147}Sm can always be maintained to 200~500 mV in this study. In only a few cases, the intensity of ^{147}Sm was lower than 200 mV. In order to check the feasibility and stability of our method for small signal ^{147}Sm, we picked up an extreme case, which had the lowest signal intensity of ^{147}Sm (*ca.* 20 mV) and the widest fluctuation range of ^{147}Sm among 131 samples in this work. It was a rock standard (BCR-2, No.7 in Table 5), which included 195 cycles with 4 outliers. As shown in Fig. 4, the corrected ^{143}Nd/^{144}Nd ratios were stable and accurate in spite of the intensity of ^{147}Sm showed wide fluctuation range from 20 to 211 mV. Especially, corrected average value of ^{143}Nd/^{144}Nd ratio was not found to be abnormal, even the intensity of ^{147}Sm was as low as 20~35 mV.

3.4 Stability of ^{145}Nd/^{144}Nd ratio

Sm is a rare-earth element with seven naturally occurring isotopes. Of these ^{147}Sm, ^{148}Sm and ^{149}Sm are all radioactive, but the latter two have such long half-lives (about 10^{16} yr) so that they are not capable of producing measurable variations in the daughter isotopes of ^{144}Nd and ^{145}Nd.[1] Therefore, ^{145}Nd/^{144}Nd ratio is regarded as constant in nature.[3–6,11,15] The mass-bias corrected value for ^{145}Nd/^{144}Nd is a good indicator to check whether ^{144}Sm can be accurately subtracted from mixed intensity of 144 (^{144}Sm + ^{144}Nd). Therefore, in this study, the ^{145}Nd/^{144}Nd ratio is employed as internal invariant and canonical value to evaluate the feasibility of our method.[3–6]

As shown in Fig. 5a, our normalized ^{145}Nd/^{144}Nd value is 0.348410 ± 0.000007 (2 SD, $n = 88$) in mixed standard JNdi-1 and LRIG, after isobaric interference correction, consistent with the reported value of 0.348405~0.348419 obtained by MC-ICP-MS and TIMS.[3–6,11,15] Also, as shown in Fig. 5b, corrected ^{145}Nd/^{144}Nd value is 0.348409 ± 0.000009 (2 SD, $n = 43$) in actual silicate reference rock samples from USGS and GSJ, agreeing well with reported values. These results support that our method is accurate and stable.

3.5 Isobaric interference of ^{144}Sm on ^{144}Nd

As noted in previous research,[4–6] isobaric interferences on Nd isotopes are principally caused by Ce (^{142}Ce on ^{142}Nd) and Sm (^{144}Sm on ^{144}Nd, ^{148}Sm on ^{148}Nd and ^{150}Sm on ^{150}Nd). Because we

This journal is © The Royal Society of Chemistry 2011

J. Anal. At. Spectrom., 2011, **26**, 2012–2022 | 2017

Table 5 CRMs determined using TIMS without Nd and Sm separation compared with published TIMS analyses of purified Nd fractions

| CRM | TIMS | | | | | Recommended value | |
	Fraction	β_{Sm}	β_{Nd}	$^{143}Nd/^{144}Nd$ (±S.E)	$^{145}Nd/^{144}Nd$ (±S.E)	$^{143}Nd/^{144}Nd$ (Fluctuating Range)	Sm/Nd
GSP-2	REE[1]	0.378	0.112	0.511360(3)	0.348412(2)	0.511353–0.511389[10,19,21]	0.127[29]
	REE[2]	0.320	0.042	0.511359(2)	0.348407(1)		
	Mean	0.349	0.077	0.511359	0.348410		
JG-3	REE[1]	0.437	0.187	0.512619(4)	0.348411(3)	0.512606–0.512644[9,24]	0.186[29]
	REE[2]	0.474	0.271	0.512610(7)	0.348411(5)		
	Mean	0.456	0.229	0.512615	0.348411		
JR-3	REE[1]	0.284	0.060	0.512670(6)	0.348403(4)	0.512666–0.512685[9]	0.201[29]
	REE[2]	0.423	0.175	0.512681(3)	0.348412(2)		
	Mean	0.354	0.118	0.512675	0.348408		
JG-1a	REE[1]	0.329	0.058	0.512373(6)	0.348405(4)	0.512331–0.512385[9,17,18,26]	0.233[29]
	REE[2]	0.448	0.187	0.512380(5)	0.348408(3)		
	Mean	0.389	0.123	0.512376	0.348407		
BHVO-2	REE[1]	0.494	0.228	0.512982(4)	0.348411(2)	0.512957–0.512995[9,10,19,21]	0.245[10]
	REE[2]	0.287	0.052	0.512988(3)	0.348410(2)		
	Mean	0.390	0.140	0.512985	0.348410		
JA-3	REE[1]	0.417	0.197	0.512830(6)	0.348404(4)	0.512829–0.512859[9]	0.248[29]
	REE[2]	0.323	0.048	0.512849(3)	0.348408(2)		
	Mean	0.370	0.122	0.512840	0.348406		
W-2	REE[1]	0.445	0.163	0.512514(4)	0.348407(3)	0.512509–0.512538[10,16,17,20]	0.254[29]
	REE[2]	0.413	0.143	0.512512(6)	0.348407(4)		
	Mean	0.429	0.153	0.512513	0.348407		
JGb-1	REE[1]	0.228	0.095	0.512669(7)	0.348408(5)	0.512624–0.512672[9,16,18,26,27]	0.266[29]
	REE[2]	0.054	0.293	0.512659(9)	0.348420(6)		
	Mean	0.141	0.194	0.512664	0.348414		
JGb-2	REE[1]	0.275	0.097	0.512226(5)	0.348407(3)	0.512210–0.512240[9]	0.271[29]
	REE[2]	0.371	0.120	0.512218(6)	0.348413(4)		
	Mean	0.323	0.109	0.512222	0.348410		
JR-2	REE[1]	0.429	0.171	0.512921(5)	0.348413(3)	0.512900–0.512918[9,27]	0.275[29]
	REE[2]	0.500	0.238	0.512914(5)	0.348408(4)		
	Mean	0.464	0.205	0.512917	0.348411		
JG-2	REE[1]	0.338	0.084	0.512244(9)	0.348408(7)	0.512210–0.512240[9,24]	0.313[29]
	REE[2]	0.311	0.055	0.512232(5)	0.348414(4)		
	Mean	0.325	0.070	0.512238	0.348411		
BIR-1	REE[1]	0.330	0.055	0.513091(5)	0.348413(3)	0.513064–0.513107[9,10,16,17]	0.460[29]
	REE[2]	0.098	0.127	0.513081(6)	0.348414(4)		
	REE[3]	0.098	0.176	0.513077(6)	0.348407(4)		
	REE[4]	0.335	0.066	0.513088(8)	0.348408(6)		
	REE[5]	0.268	0.089	0.513085(5)	0.348409(3)		
	REE[6]	0.139	0.148	0.513079(9)	0.348418(3)		
	REE[7]	0.302	0.061	0.513093(9)	0.348408(6)		
	REE[8]	0.160	0.080	0.513080(9)	0.348426(7)		
	Mean ± 2SD	0.216	0.100	0.513084(12)	0.348412(13)		
BCR-2	REE[1]	0.271	0.053	0.512628(4)	0.348405(3)	0.512622–0.512654[9,10,19,20,21]	0.229[10]
	REE[2]	0.274	0.068	0.512631(4)	0.348406(2)		
	REE[3]	0.234	0.098	0.512624(4)	0.348405(3)		
	REE[4]	0.374	0.070	0.512624(3)	0.348409(2)		
	REE[5]	0.478	0.217	0.512630(4)	0.348411(2)		
	REE[6]	0.484	0.216	0.512631(3)	0.348408(2)		
	REE[7]	0.109	0.216	0.512624(3)	0.348406(2)		
	REE[8]	0.095	0.140	0.512636(3)	0.348409(2)		
	REE[9]	0.480	0.229	0.512633(4)	0.348407(3)		
	REE[10]	0.497	0.244	0.512635(3)	0.348406(3)		
	REE[11]	0.179	0.042	0.512628(6)	0.348407(4)		
	REE[12]	0.493	0.265	0.512639(6)	0.348409(4)		
	REE[13]	0.475	0.228	0.512630(4)	0.348407(2)		
	Mean ± 2SD	0.342	0.161	0.512630(10)	0.348407(4)		

are interested in the radiogenic $^{143}Nd/^{144}Nd$ ratios in this study, correction of interference of ^{142}Ce on ^{142}Nd is not performed. Moreover, BaO^+ and BaN^+, which is $^{130}Ba^{14}N^+$ on ^{144}Nd, $^{132}Ba^{14}N^+$ on ^{146}Nd, $^{130}Ba^{16}O^+$ on ^{146}Nd, $^{132}Ba^{16}O^+$ on ^{148}Nd and $^{134}Ba^{16}O^+$ on ^{150}Nd, are regarded as potential interferences in MC-ICP-MS.[4–6] Of these, $^{130}Ba^{14}N^+$ and $^{130}Ba^{16}O^+$ are thought to be the most important interferences on ^{144}Nd and ^{146}Nd for mass fractionation correction. In order to verify the impact status of

BaO^+ and BaN^+ by using TIMS, 20 μg $BaCl_2$ is loaded on the Re filament following the loading method of Nd. Mass scanning is performed to check the intensity of BaO^+ and BaN^+ when the signal intensity of $^{138}Ba^+$ is higher than 20 V. No BaO^+ and BaN^+ signals are found. Hence, we conclude that all isobaric interferences come from Sm.

How to accurately correct the ^{144}Sm interference on ^{144}Nd is the major technical difficulty for precise measurements of

Table 6 CRMs determined by TIMS after complete Nd and Sm separation using traditional two-step chromatographic method

CRM	Analysis number	$^{143}Nd/^{144}Nd$ ($\pm$S.E)
GSP-2	a	0.511371(2)
	b	0.511364(5)
	Mean	0.511368
JG-3	a	0.512627(3)
	b	0.512628(3)
	Mean	0.512628
JR-3	a	0.512685(2)
	b	0.512673(3)
	Mean	0.512679
JG-1a	a	0.512374(4)
	b	0.512373(4)
	Mean	0.512374
BHVO-2	a	0.512987(3)
	b	0.512982(3)
	Mean	0.512985
JA-3	a	0.512851(3)
	b	0.512849(5)
	Mean	0.512850
W-2	a	0.512516(3)
	b	0.512508(4)
	Mean	0.512512
JGb-1	a	0.512653(4)
	b	0.512660(4)
	Mean	0.512657
JGb-2	a	0.512212(6)
	b	0.512220(6)
	Mean	0.512216
JR-2	a	0.512924(5)
	b	0.512921(6)
	Mean	0.512923
JG-2	a	0.512235(3)
	b	0.512234(2)
	Mean	0.512235
BIR-1	a	0.513082(5)
	b	0.513093(4)
	Mean	0.513088
BCR-2	a	0.512640(3)
	b	0.512633(4)
	Mean	0.512636
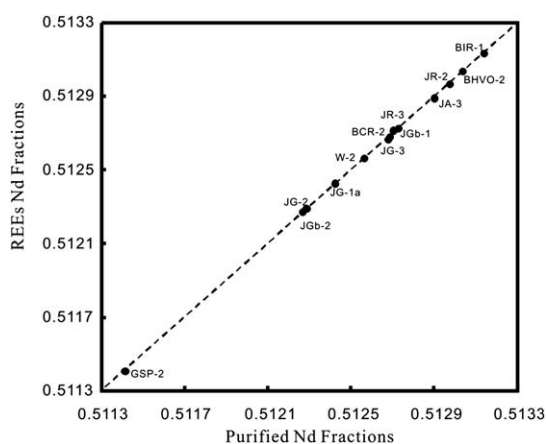
Fig. 3 Comparison of $^{143}Nd/^{144}Nd$ average value between purifed Nd fractions and REEs fractions.

$^{143}Nd/^{144}Nd$ ratio. In previous investigations, three methods were presented:

[1]. The first approach assumed that both Sm and Nd have identical mass biases, which would be feasible for isobaric interference correction when only small Sm exists in the Nd fraction after chemical separation. For instance, Yang et al.[31] obtained precise $^{143}Nd/^{144}Nd$ data using Neptune without considering mass bias differences between Sm and Nd even when the Sm/Nd ratio was up to 0.04. However, this method is unsuitable for TIMS analysis due to the great discrepancy of mass fractionation factor in both Sm and Nd. As to TIMS analysis, the ionization temperature of Sm is lower than the Nd resulting in significant difference in mass fractionation factors. Most β_{Sm}/β_{Nd} ratios are higher than 4 and even reach to 24 during Nd isotope analysis in this study. Hence, accurate and precise $^{143}Nd/^{144}Nd$ ratio using TIMS can be obtained unless the $^{147}Sm/^{144}Nd$ ratio is near to 0.[8–18]

[2]. An iterative approach for the Sm correction was presented by Foster and Vance.[4] The basic principle was to obtain a stable value of $^{146}Nd/^{144}Nd$ ratio after several iterations for various Sm/Nd ratios prior to normalizing the $^{143}Nd/^{144}Nd$ ratio using the exponential law. They pointed out that four iterations were needed for a Sm/Nd ratio of around 0.2, while 10–15 iterations were required for a Sm/Nd ratio as high as 1.0.

[3]. The β_{Sm} value can be directly obtained from the $^{147}Sm/^{149}Sm$ ratio on the sample itself and then it is applied to the isobaric interference correction of ^{144}Sm on ^{144}Nd.[5,6] However, to the best of our knowledge, no well-accepted corrected method using TIMS is presented so far.

Similar to MC-ICP-MS, measuring the mass fractionation factor of Sm (β_{Sm}) for natural sample is the requisite of accurate correction in TIMS analysis. We employed method 3 to perform all measurements for natural silicate rock sample. Thus, to select the suitable $^{147}Sm/^{149}Sm$ and $^{147}Sm/^{144}Sm$ ratios is the key issue. Generally, the $^{147}Sm/^{149}Sm$ and $^{147}Sm/^{144}Sm$ ratios of high purity Sm standard solution or actual rock sample may be regarded as the suitable value. Hence, we firstly cited and compared the reported values in Table 7 to apply artificial mixed standard JNdi-1. Twenty-four measurements for mixed JNdi-1 with different Sm/Nd ratios (0.3, 0.5, 0.7 and 1.0), with six runs in each measurement, were carried out and corrected using different $^{147}Sm/^{149}Sm$ and $^{147}Sm/^{144}Sm$ values. As shown in Fig. 6, the corrected $^{143}Nd/^{144}Nd$ ratios using the values of Chang[28] and Wasserburg[15] are nearly identical with the reported ratio of 0.512115,[27] show excellent reproducibility. Especially, the average $^{143}Nd/^{144}Nd$ ratio of 0.512112 corrected using the values of Chang et al.[28] is almost identical to the reported value (0.512115).[27] The average of corrected $^{143}Nd/^{144}Nd$ ratios using the values of Lugmair et al.,[14] Hidaka et al.[22] and Maas and McCulloch[23] are significantly lower than the reported ratio with poor external precision. Such discrepancy is most likely attributed to the unsuitable normalization because their reported Sm isotopic ratios were obtained using an assuming constant value to normalize the others. Rigorous determination of the isotopic composition of an element in a sample should avoid any assumptions, in particular, assumptions about the isotopic composition itself. In contrast, the $^{147}Sm/^{149}Sm$ and $^{147}Sm/^{144}Sm$ values of from Chang[28] are more reliable as they originated from a calibrated measurement using gravimetric synthetic mixtures of separated isotopes of samarium and underwent the severe instrumental corrections without any assumption.
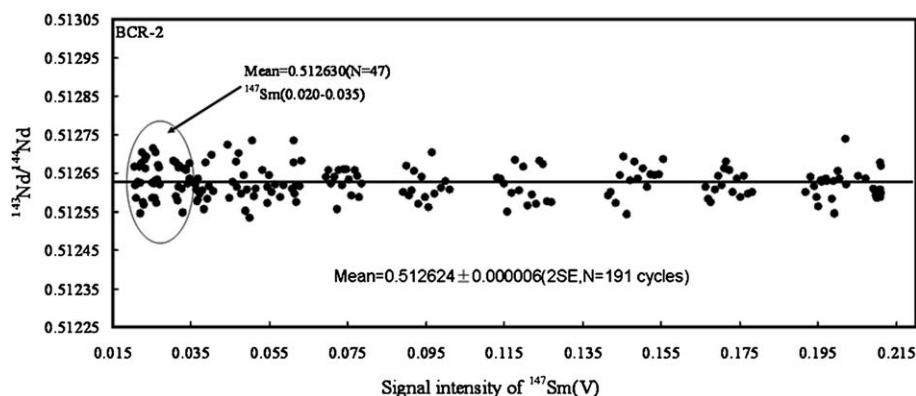
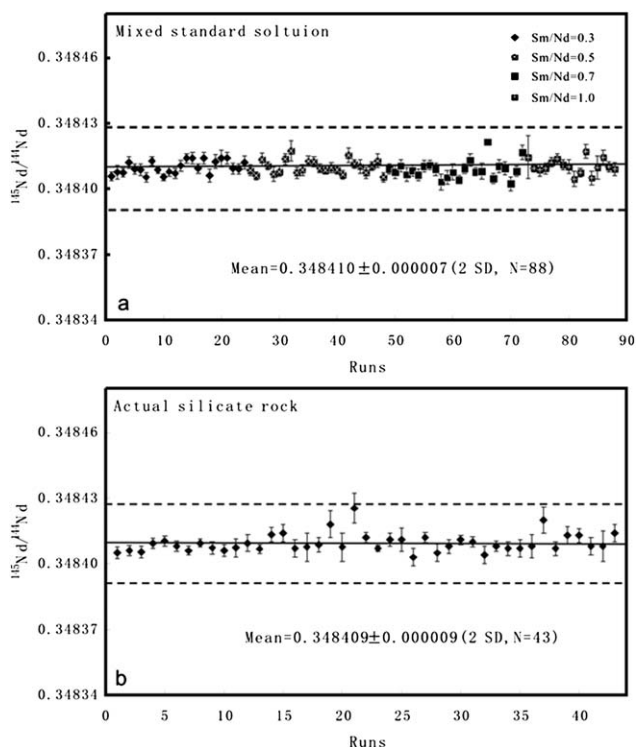**Fig. 4** Relationship between the [147]Sm intensity and corrected [143]Nd/[144]Nd.

Fig. 5 Corrected [145]Nd/[144]Nd ratios for each runs **a.** artificial mixed standard JNdi-1 and LRIG; **b.** actual silicate rock from USGS and GSJ.

3.6 Potential application and limitation of this method

Neodymium isotopic compositions of sediments most likely reflect their source materials because Nd isotope ratios are not significantly altered by the lower temperature processes such as

weathering, transportation and deposition. Thus, [143]Nd/[144]Nd ratios are useful to reconstruct paleo-environment from loess or fine-grained clastic sediment in quaternary and tertiary period. However, a large number of samples and data are required to extract high-resolution paleo-environment records.[32–37] Generally, approximately 100 samples should be determined at least for one sedimentary column or sedimentary section. Our new method is simpler and less time-consuming, providing a rapid analytical protocol to precisely determine [143]Nd/[144]Nd ratio of natural rock samples. In addition, we can fully make use of the previous method to obtain purified Sr and REE from single-column chemistry.[18–21,24–26] This method significantly simplifies the Sm–Nd separation procedure and allows larger sample throughput. Therefore, our new method is especially useful for the studies requiring a large number of samples.

Despite suitability in application to most natural silicate rocks, this new method has several limitations. Firstly, it may be not suitable to samples with Sm/Nd ratio higher than 1.0, such as garnet and zircon. More strict experiments must be performed to assess the feasibility of our method to above special minerals. Secondly, we employ Nd^+ manner to determine Nd isotope which cannot provide satisfactory precision for small sample sizes of less than 50 ng. However, this problem is easily settled using NdO^+ manner combined with traditional chemistry procedure, even to 1 ng of Nd.[9,10] Thirdly, this new method is suitable for precise determination [143]Nd/[144]Nd for un-spiked samples, but Sm and Nd concentrations cannot be determined in the same aliquot simultaneously because [147]Sm/[149]Sm must be employed to calculate β_{Sm}. However, accurate [147]Sm/[144]Nd ratio is indispensable to calculate $\varepsilon Nd(t)$ which is the most useful indicator for tracing researches. This limitation can be partly overcome by deploying quadrupole-based or sector field ICP-MS for determining the Sm/Nd ratio.[38–41] As a result of limitations in

Table 7 Compilation of published Sm isotopic ratios

| [147]Sm/[149]Sm	[147]Sm/[144]Sm	Instrument	Reporter	Comment
1.08583	4.87090	MAT262(TIMS)	T.L Chang(2002)	No mass fractionation correction
1.08507	4.87703	Lunatic(TIMS)	G.J.Wasserburg(1981)	Mass fractionation correction to [148]Sm/[154]Sm = 0.49419
1.08549	4.87948	Lunatic(TIMS)	G.W. Lugmair(1975)	Mass fractionation correction to [147]Sm/[152]Sm = 0.56081
1.08557	4.87869	VG54-30(TIMS)	H. Hidaka(1995)	Mass fractionation correction to [147]Sm/[152]Sm = 0.56083
1.08512	4.87865	MAT261(TIMS)	R.Maas (1990)	Mass fractionation correction to [147]Sm/[152]Sm = 0.56083
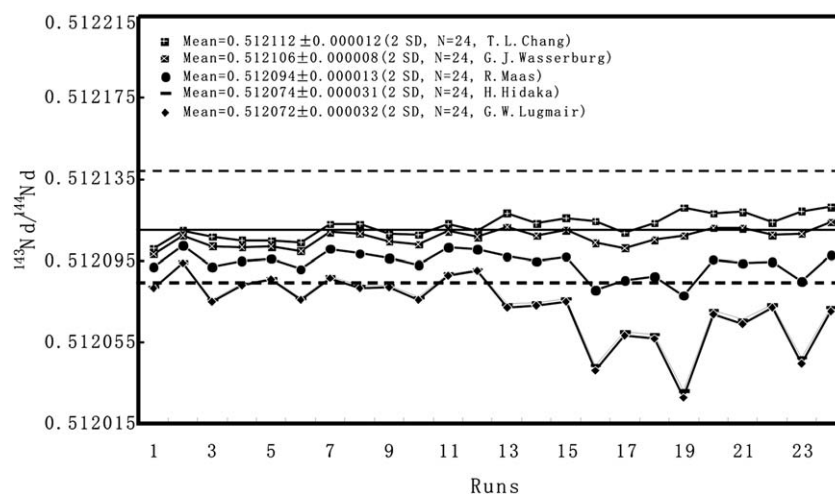
Fig. 6 The corrected results with different corrected parameters.

the precision with which this can be typically accomplished, for old rocks, however, the traditional ID-TIMS technique is still preferable to minimize the error magnification of εNd (t).

4. Conclusions

Nd isotope ratios of CRMs covering a wide range of Sm/Nd ratios (0.13– 0.46) and $^{143}Nd/^{144}Nd$ ratios (0.5113–0.5130), were measured using Triton TIMS without Sm and Nd separation. The precision and accuracy of Nd isotope ratios using this new method are as good as those obtained by classical TIMS or MC-ICP-MS methods after Sm–Nd separation. $^{149}Sm/^{147}Sm$ ratio of 1.08583 and $^{147}Sm/^{144}Sm$ ratio of 4.87090 are used to subtract isobaric interference and calculate β_{Sm}. This method of correcting Sm interferences is viable even for those samples with Sm/Nd ratio up to 1.0, indicating that Sm–Nd separation is not a requisite for precise Nd isotopic analysis. This quick, simple new method has great potential for improving sample throughput in Nd isotope analysis.

References

1 A. P. Dickin, *Radiogenic Isotope Geology*, Cambridge University Press, 2004.
2 G. Faure, *Isotope Principles and Applications* third edition John Wiley & Sons, Inc, 2005.
3 B. Luais, P. Telouk and F. Albarede, *Geochim. Cosmochim. Acta*, 1997, **61**, 4847–4854.
4 G. L. Foster and D. Vance, *J. Anal. At. Spectrom.*, 2006, **21**, 288–296.
5 C. R. M. McFarlane and M. T. McCulloch, *Chem. Geol.*, 2007, **245**, 45–60.
6 Y. H. Yang, F. Y. Wu, L. W. Xie and Y. B. Zhang, *Anal. Lett.*, 2010, **43**, 142–150.
7 M. F. Thirlwall, *Chem. Geol.*, 1991, **94**, 13–22.
8 M. Griselin, J. C. Van Belle, C. Pomies, P. Z. Vroon, M. C. van Soest and G. R. Davies, *Chem. Geol.*, 2001, **172**, 347–359.
9 C. F. Li, F. K. Chen and X. H. Li, *Int. J. Mass Spectrom.*, 2007, **266**, 34–41.
10 Z. Y. Chu, F. K. Chen, Y. H. Yang and J. H. Guo, *J. Anal. At. Spectrom.*, 2009, **24**, 1534–1544.
11 G. Caro, B. Bourdon, J. L. Birck and S. Moorbath, *Geochim. Cosmochim. Acta*, 2006, **70**, 164–191.
12 M. Sharma and C. Chen, *Precambrian Res.*, 2004, **135**, 315–329.
13 R. Andreasen and M. Sharma, *Int. J. Mass Spectrom.*, 2009, **285**, 47–59.
14 G. W. Lugmair, N. B. Scheinin and K. Marti, *Proc. 6th Lunar Sci. Conf*, 1975, 1419–1429.
15 G. J. Wasserburg, S. B. Jacobsen, D. J. DePaolo, M. T. McCulloch and T. Wen, *Geochim. Cosmochim. Acta*, 1981, **45**, 2311–2323.
16 C. Pin, D. Briot, C. Bassin and E. Poitrasson, *Anal. Chim. Acta*, 1994, **298**, 209–217.
17 C. Pin, J. Francisco and S. Zaldueguí, *Anal. Chim. Acta*, 1997, **339**, 79–89.
18 C. Na, T. Nakano, K. Tazawa, M. Sakagawa and T. Ito, *Chemical Geology (Isotope Geoscience Section)*, 1995, **123**, 225–237.
19 D. Weis, B. Kieffer, C. Maerschalk, J. Barling, J. D. Jong, G. A. Williams, D. Hanano, W. Pretorius, N. Mattielli, J. S. Scoates, A. Goolaerts, R. M. Friedman and J. B. Mahoney, *Geochem., Geophys., Geosyst.*, 2006, DOI: 10.1029/2006GC001283.
20 Y. H. Yang, H. F. Zhang, Z. Y. Chu, L. W. Xie and F. Y. Wu, *Int. J. Mass Spectrom.*, 2010, **290**, 120–126.
21 I. Raczek, K. P. Jochum and A. W. Hofmann, *Geostand. Geoanal. Res.*, 2003, **27**, 173–179.
22 H. Hidaka, M. Ebihara and M. Shima, *Anal. Chem.*, 1995, **67**, 1437–1441.
23 R. Maas and M. T. McCulloch, *Chem. Geol.*, 1990, **88**, 301–315.
24 Y. Arakawa, *Geochem. J.*, 1992, **26**, 105–109.
25 Y. Orihashi, J. Maeda, R. Tanaka, R. Zeniya and K. Niida, *Geochem. J.*, 1998, **32**, 205–211.
26 T. Miyazaki and K. Shuto, *Geochem. J.*, 1998, **32**, 345–350.
27 T. Tanaka, S. Togashi, H. Kamioka, H. Amakawa, H. Kagami, T. Hamamoto, M. Yuhara, Y. Orihashi, S. Yoneda, H. Shimizu, T. Kunimaru, K. Takahashi, T. Yanagi, T. Nakano, H. Fujimaki, R. Shinjo, Y. Asahara, M. Tanimizu and C. Dragusanu, *Chem. Geol.*, 2000, **168**, 279–281.

This journal is © The Royal Society of Chemistry 2011

J. Anal. At. Spectrom., 2011, **26**, 2012–2022 | 2021

28 T. L. Chang, M. T. Zhao, W. J. Liu, J. Wang and Q. Y. Qian, *Int. J. Mass Spectrom.*, 2002, **218**, 167–172.
29 P. Dulski, *Geostand. Geoanal. Res.*, 2001, **25**, 87–125.
30 R. L. Korotev, *Geostand. Geoanal. Res.*, 1996, **20**, 217–245.
31 Y. H. Yang, H. F. Zhang, L. W. Xie and F. Y. Wu, *Chin J Anal Chem.*, 2007, **35**, 71–74.
32 Y. X. Wang, J. D. Yang, J. Chen, K. J. Zhang and W. B. Rao, *Palaeogeogr., Palaeoclimatol., Palaeoecol*, 2007, **249**, 351–361.
33 T. Pettke, A. N. Halliday, C. M. Hall and D. K. Rea, *Earth Planet. Sci. Lett.*, 2000, **178**, 397–413.
34 S. Gallet, B. M. Jahn and M. Torii, *Chem. Geol.*, 1996, **133**, 67–88.
35 B. M. Jahn, S. Gallet and J. M. Han, *Chem. Geol.*, 2001, **178**, 71–94.
36 Y. Yokoo, T. Nakano, M. Nishikawa and H. Quan, *Chem. Geol.*, 2004, **204**, 45–62.
37 J. M. Sun, *Earth Planet. Sci. Lett.*, 2005, **240**, 454–466.
38 C. Pin, *J. Anal. At. Spectrom.*, 1995, **10**, 93–98.
39 P. Montero and F. Bea, *Anal. Chim. Acta*, 1998, **358**, 227–233.
40 M. D. Orazioa and S. Tonarinib, *Anal. Chim. Acta*, 1997, **351**, 325–335.
41 P. J. Patchett, A. F. Embry, G. M. Ross, B. Beauchamp, J. C. Harrison, U. Mayr, C. E. Isachsen, E. J. Rosenberg and G. O. Spence, *J. Geol.*, 2004, **112**, 39–57.